Synthesis and antimicrobial properties of new chitosan derivatives containing guanidinium groups

Ahmed Salama, Mohamed Hasanin, Peter Hesemann

Synthesis and antimicrobial properties of new chitosan derivatives containing guanidinium groups

Ahmed Salama[1,2,]* Mohamed Hasanin[2] and Peter Hesemann[1]

[1]Institut Charles Gerhardt de Montpellier, UMR CNRS 5253 Université de Montpellier-CNRS-ENSCM, Place Eugène Bataillon, 34095 Montpellier Cedex 05, France

[2]Cellulose and Paper Department, National Research Centre, 33 El-Behouth St., Dokki, P.O. 12622, Giza, Egypt

*corresponding author: Ahmed_nigm78@yahoo.com
Tel: 00201008842629

Graphical Abstract
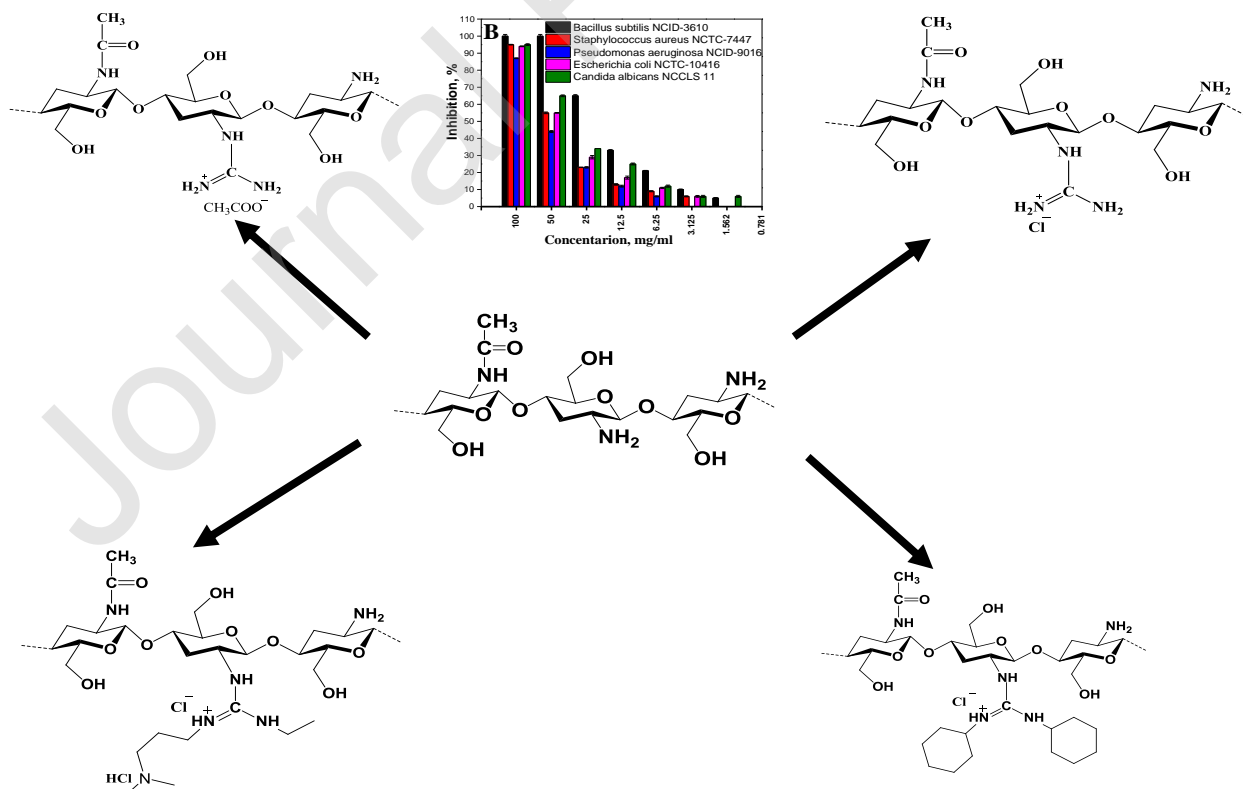
Highlights

- New chitosan derivatives bearing guanidinium functions were prepared and characterized.
- The four derivatives displayed improved antimicrobial activity in comparison with neat chitosan.
- Biosourced and renewable chitosan derivatives could be applied as antimicrobial surfaces.

Abstract

New chitosan derivatives bearing guanidinium functions were synthesized following different synthesis strategies. *N*-guanidinium chitosan acetate and *N*-guanidinium chitosan chloride were synthesized by direct reaction between chitosan and cyanamide in the presence of scandium(III) triflate. The synthesis of *N*-guanidinium chitosan *(N,N'*-dicyclohexyl) chloride and *N*-guanidinium chitosan (*N*-(3-dimethylaminopropyl)-*N'*-ethyl hydrochloride) chloride involved the reaction of chitosan with carbodiimides in ionic liquid. The chitosan derivatives were characterized by analytical techniques including ^{13}C solid state NMR, FT-IR spectroscopies, thermogravimetry and elemental analysis. The antimicrobial properties of chitosan and the new derivatives were investigated using the minimal inhibitory concentration (MIC) technique. All new guanylated chitosan derivatives displayed high antimicrobial activity in comparison with neat chitosan. The N-guanidinium chitosan acetate reduced the time required for killing to half in comparison with chitosan and recorded MIC values less than 3.125 mg/ml against all assayed microorganisms. This work opens new perspectives for using chitosan derivatives as antimicrobial surfaces.

1- Introduction

The antimicrobial resistance toward conventional antibiotics can often lead to serious diseases in humans (Sahariah, Másson, & Meyer, 2018). Because of the increased emergence of antibiotic resistant microbial, different innovative techniques to combat bacteria have been established. A novel method uses natural and biodegradable polymers as antimicrobials for the prevention the growth of microorganisms.   Among them, polysaccharides have recently emerged as promising candidates for the development of functional biomaterials due to their low cost, non-toxicity, bio-degradability and their virtually unlimited availability (Salama, 2019; Salama, Abou-Zeid, Cruz-Maya, & Guarino, 2020). Polysaccharides with antimicrobial properties were proposed as potential antibiotic and microbial resistant materials for biomedical applications (Salama, 2017).

In this context, chitin, a biopolymer derived from the exoskeleton of insects and crustaceans, can be chemically converted to its partially deacetylated form, called chitosan (Hassan, Salama, El-ziaty, & El-sakhawy, 2019). The chemical structure of chitosan permits a variety of chemical modifications to synthesize novel derivatives containing functional groups, such as cationic or other hydrophilic and hydrophobic moieties (Holappa et al., 2004; Sahariah et al., 2015). Neat chitosan is insoluble in aqueous medium. In acidic medium, the amino groups are converted to ammonium cations. Moreover, these amino groups in chitosan increase the hydrophilicity and improve its water solubility in acidic aqueous solutions. Chitosan has been reported as a promising sustainable material for different applications such as adsorption (Monier, Abdel-Latif, & Youssef, 2018), biomineralization (Salama, 2018) and drug delivery (Salama & El-Sakhawy, 2014). Hence, chitosan is a highly versatile biopolymer

3

allowing a variety of chemical modifications. It is noteworthy that chitosan displays weak inherent antimicrobial activity which disappeared with many microbial strains. Native chitosan offered limited ability for killing microorganisms, where the lone pair of electrons on amino groups is controlled via unique structure. For this reason, many researchers tried to improve the antimicrobial activity of chitosan via chemical modifications (Sahariah et al., 2015; Shehabeldine & Hasanin, 2019). The effect of the cationic charge on the antimicrobial activity of chitosan derivatives has been matter of various studies. The cationic charges are responsible for binding of chitosan to anionic components in the bacterial membrane through electrostatic attractions followed by the rupture of the cell membrane permeability control. Its ability to inhibit microbial growth is observed only in acidic medium, where the polymer is carrying positive charges (Salama & Hesemann, 2018a). Furthermore, the antimicrobial properties of chitosan can be increased not only through functionalization with functional groups such as cationic alkylammonium, guanidinium, anionic carboxylate functions, or thiol-containing groups but also with more hydrophobic substituents, such as alkyl, phenyl and benzyl groups (Sahariah et al., 2015; Sahariah & Másson, 2017).

As already mentioned, the elaboration of chitosan with enhanced antibacterial activity via derivatization with cationic moieties attracted considerable attention. For example, Rúnarsson *et al.* reported that the presence of ammonium or pyridinium groups on the chitosan chains improved antibacterial activity compared to neat chitosan (Vidar Rúnarsson et al., 2010). Moreover, surface-quaternized derivatives of chitosan containing high charge density together with the presence of hydrophobic benzyl groups inhibited the growth of different bacteria compared with derivatives containing propyl groups (Wiarachai, Thongchul, Kiatkamjornwong, & Hoven, 2012).

The guandine/guanidinium entity is an important functional group in biochemistry as biological receptors especially for RNA. Due to its high pKa value, guanidine exclusively exists in aqueous solution in its protonated form, *i.e.* the guanidinium cation. The distinctive property of the guanidinium cation is the ability to interact with various anionic functional groups *via* the formation of ion pairs combined with strong hydrogen bonding. The introduction of guanidinium groups into chitosan *via* reaction between chitosan and arginine was studied by Zhang *et al*. (Zhang, Duan, Wang, & Bian, 2015). Hu *et al*. investigated the introduction of the guanidine moiety on the chitosan backbone *via* reaction with aminoiminomethanesulfonic acid (Hu et al.,

4

2007). In our previous work, the formation of *N*-guanidinium chitosan acetate was achieved through direct guanylation of chitosan with cyanamide in presence of scandium (III) (Salama & Hesemann, 2020). We used this material for the formation of microhybrids *via* a sol gel technique involving 3-glycidoxypropyl trimethoxysilane. The resulting material was used as new adsorbent for water purification from organic dyes (Salama & Hesemann, 2018b). Another study focused on the formation of ionic composite materials via the sol-gel reaction with 3-(trihydroxysilyl)-1-propanesulphonic acid. The resulting ionic microhybrids were also successfully used as new adsorbents for water purification (Salama & Hesemann, 2018a).

In this study, we investigated the impact of guanidinium groups on the biological activity of guanylated chitosan derivatives. Besides, guanylated chitosan obtained via scandium(III) catalyzed guanylation reaction (*vide supra*), we synthesized new guanylated chitosan materials by reacting chitosan with carbodiimides in ionic liquid media. The resulting guanylated chitosan derivatives were characterized using various techniques. The impact of the guanidinium moieties and the counter anion in the study of antibacterial activity was the main objective of this study. The antimicrobial profile was monitored via the estimation of minimal inhibitory concentration (MIC) and time required for killing, to evaluate the bioavailability and antimicrobial efficiency of the materials.

2. Experimental part

2.1. Materials

Medium molecular weight chitosan (degree of deacetylation, 75-85%), cyanamide, *N*,*N*′-dicyclohexylcarbodiimide, *N*-(3-Dimethylaminopropyl)-*N*′-ethylcarbodiimide hydrochloride and scandium(III) triflate were obtained from Sigma-Aldrich. 1-Butyl-3-methylimidazolium chloride (BMIM Cl) was purchased from *io-li-tec*. All other chemicals of analytical grade and used without further purification. All aqueous solutions were prepared using deionized water. All reagents and microbial media were of analytical grade and used without any previous treatment.

2.2. Syntheses

Synthesis of *N*-guanidinium chitosan acetate (B) and *N*-guanidinium chitosan chloride (C).

Synthesis of materials B and C was performed by preparing 10 ml of a 2% solution of chitosan (A) in 2% acetic acid, or 2% hydrochloric acid, in case of material B and C, respectively. These solutions were mixed with 0.084 g cyanamide (2 mmol) and 0.03 g (60 nmol) of scandium(III) triflate. The solution was stirred at 100°C for 48 h, the resulting mixture was precipitated and washed several times with acetone. Material B from acetic acid and material C isolated from hydrochloric acid were freeze-dried to obtain the pure products B and C as a light brown solid.

Synthesis of N-guanidinium chitosan *(N,N′*-dicyclohexyl) chloride (D) and N-guanidinium chitosan (*N*-(3-dimethylaminopropyl)-*N*'-ethyl hydrochloride) chloride (E)

Chitosan (0.1 g) was dissolved in BMIM Cl (10 g) at 90 ºC under magnetic stirring for 2 days. The reaction of chitosan with *N,N′*-dicyclohexylcarbodiimide or N-(3-Dimethylaminopropyl)-N'-ethylcarbodiimide hydrochloride (1.2 mmole) was allowed to proceed at 100 ºC for 2 days. The products were isolated by precipitation in 450 mL methanol. The polymers were isolated by filtration and washed three times with 50 mL aliquots of methanol. The collected chitosan derivatives (D and E) were freeze-dried and separated as brown solids.

2.3. Characterization methods.

Elemental analysis. EA was done with an Elemental Vario Micro Cube apparatus.

Solid state NMR spectroscopy. ^{13}C Cross Polarization Magic Angle Spinning (CP/MAS) was used to obtain a high signal-to-noise ratio with 5 ms contact time and 5 s recycling delay.

FT-IR Spectroscopy. The attenuated total reflectance Fourier transform infrared (ATR-FTIR) spectra of materials were obtained using a Thermo Nicolet FT-IR Avatar 320 with a diamond crystal. Spectra were recorded from 500 to 4000 cm^{-1}.

Thermogravimetric Analysis. TGA measurements were carried out with a NETZSCH STA 409 PC instrument. All materials were burned under air between 25 and 800 °C at a heating rate of 5 °C/min.

2.4. Antimicrobial studies

The antimicrobial studies were carried out to evaluate the antimicrobial behavior of the new chitosan derivatives. Turbidimetric method was used to judge the antimicrobial activity according to the procedure described by J. Balouiri et. al. (Balouiri, Sadiki, & Ibnsouda, 2016). The minimal inhibitory concentration (MIC) was

carried out according to our previous work (M. S. Hasanin & Moustafa, 2020). The serial dilution method was used from 100 mg/ml to 0 mg/ml as a negative control. Cultures of the following microorganisms were used in the tests: (i) Gram-negative bacteria: *Escherichia coli* (NCTC-10416) and *Pseudomonas aeruginosa* (NCID-9016); (ii) Gram-positive bacteria: *Staphylococcus aureus* (NCTC-7447) and *Bacillus subtilis* (NCID-3610); (iii) unicellular fungi: namely, *Candida albicans* (NCCLS 11) using nutrient broth medium. One colony of each microbial strain was suspended in a physiological saline solution (NaCl 0.9% in distilled water at pH 6.5). Mueller Hinton broth medium was inoculated by the above-mentioned bacterial strains and incubated individually at 37 °C for 24 h. After the incubation process, the turbidity was measured with V-630 UV–vis spectrophotometer (Jasco, Japan) at a wavelength of 530 nm, and the above concentrations were used to determine the MIC values under the same incubation conditions. The inhibition percentage was calculated according to equation (1).

$$Inhibition\ \% = \frac{Absorbance\ of\ untreated\ sample - Absorbance\ of\ treated\ sample}{Absorbance\ of\ untreated\ sample} \times 100 \qquad (1)$$

Data are expressed as mean ± standard deviation (SD) values. The data analysis was done using the Origin lab 9 professional edition program to carry out these statistical tests.

For determination the time required for killing, the assayed microorganisms strains were subjected to cultivation in the concentration of 400 cells which refers to the logarithmic growth phase. The prepared samples were diluted to 106 colony forming units (CFU) in milliliter for each microorganism strain (CFU/mL). MIC values of each microbial strain were multiplied by four times and used at initial concentration in Mueller Hinton broth media. Aliquots (100 mL) were collected from each treatment after 0, 2, 4, 6, 8, 10, 12, 14, 16, 18, 20, 22, and 24 h of incubation at 37 °C and subsequently serially diluted in phosphate-buffered saline (PBS). Microorganisms were then transferred to Mueller Hinton agar plates and incubated at 37 °C for 24 h before determining the viable results of CFU/mL (Eid et al., 2017).

3. Results and discussion

3.1 Synthesis of the chitosan derivatives.

Chemical modifications of chitosan are expected to enhance its antimicrobial activity toward bacteria. Various functional groups such as quaternary ammonium groups containing alkyl chains were generated on the chitosan chains to enhance its antimicrobial activity. These studies showed that the quaternary ammonium groups and the presence of long alkyl chains effectively control the efficacy against bacteria (Sahariah et al., 2018). The formation of guanidinium functions by reacting primary amines and cyanamide has already been reported. However, these reactions often require harsh conditions and were sometimes accompanied by the formation of secondary products which are difficult to eliminate, *e.g.* pyrazole. Short and Darby reported the formation of guanidinium salts *via* the reaction of ammonium starting materials and cyanamide at elevated temperatures and in the presence of concentrated hydrochloric acid (Short & Darby, 1967). More recently, Tsubokura *et al.* reported a new protocol requiring milder reaction conditions. This reaction strategy involved the use of scandium(III) triflate as Lewis acid catalyst (Tsubokura et al., 2014). On the other side, carbodiimides have attracted increasing attention for preparing complexes with a substituted propiolamidine group or a substituted guanidinate groups (Cao et al., 2011). Here, we used these two protocols for preparing new chitosan supported guanidinium groups as shown in scheme 1.

Scheme 1 illustrates the synthesis of the four *N*-guanidinium chitosan derivatives **B** - **E** through the reaction of chitosan **A** with cyanimide (for synthesis materials **B**, **C**) and carbodiimides (for synthesis materials **D**, **E**). The conversion of the amino groups to guanidinium functions was monitored *via* elemental analysis, FT-IR and ^{13}C CP-MAS-NMR spectroscopy as well as by TGA.

The results of elemental analysis measurements for materials **B**, **C**, **D** and **E** are given in table 1. The results indicate significant increase of the nitrogen content from 7.7 for neat chitosan to 11.06, 12.33, and 10.47 for materials **B**, **C** and **E**, respectively. However, the nitrogen content doesn't increase in material **D** may be due to the presence of two carbon rich moieties, cyclohexyl rings. These results together with the decreased values observed for carbon give a first indication for the successful formation of guanidinium moieties supported on chitosan.

3.2. FT-IR study

The functional groups of chitosan and its derivatives were confirmed by means of FTIR spectroscopy. Figure 1 a/b shows the FT-IR spectroscopy of materials **A**, **B**, **C**, **D** and **E**. The spectrum of neat chitosan **(A)** shows a broad band at around 3450 cm^{-1} which can be attributed to N-H and O-H symmetric stretching vibration and inter- and intra-molecular hydrogen bonds. The weak band at 2902 cm^{-1} is ascribed to the C-H stretch vibrations of chitosan. Moreover, the characteristic peaks at 1656 and 1580 cm^{-1} were due to the C=O stretching (amide I) and −NH stretching (amide II), respectively. All chitosan derivatives spectra showed the characteristic bands of chitosan skeleton. Besides, increasing the intensity of the adsorption band at 1630 cm^{-1} was observed in the spectrum of all derivatives **B to E** which suggests the generation of guanidinium moiety. The intensity of the band at 3450 cm^{-1} was decreased in case of materials D and E, comparing with neat chitosan, indicating a decrease in the density of guanidinium and hydroxyl groups arising from the presence of new alkyl and cyclohexyl branches. Moreover, the weak band at 2921 cm^{-1}, ascribed to the CH stretch vibrations of chitosan **A**, significantly increased in the charts **D** and **E**. This increase refers to the increasing in the CH stretch vibration which arises from the formation of N-guanidinium chitosan *(N, N′*-dicyclohexyl) chloride **D** and *N*-guanidinium chitosan (N-(3-Dimethylaminopropyl)-N'-ethyl hydrochloride) chloride **E**.

3.3. ^{13}C CP-MAS solid state NMR

The characterization of the materials via ^{13}C CP-MAS solid state NMR spectroscopy is a highly efficient tool to follow the derivatization and chemical evolution of the materials via the different guanylation reactions. We therefore performed ^{13}C CP-MAS solid state NMR experiments for the parent chitosan **A** and the new derivatives **B** - **E**. The spectra are given in the figure 2a/b. The spectra of chitosan **A** principally shows signals in the area of 55-110 ppm, due to the anhydroglucose units. More specifically, the signals at 55 ppm can be attributed to the CH$_2$ (C6), whereas the signal at 70 ppm is due to a superposition of the C2, C3, and C5 carbon centers. The signals of the C1 and C4 carbon are shifted to lower field (80 and 104 ppm) due to strong electron withdrawing effect of neighboring oxygen atoms. Finally, the signals of low intensity

9

observed at 25 and 175 ppm are due to residual acetyl groups and reflect the partial deacetylation of chitosan.

In the spectrum of material **B**, an additional signal at 160 ppm can be assigned to the carbon centers of the newly formed guanidinium groups (C9). Furthermore, the signal at 180 ppm can be ascribed to acetate counter ions. Hence, ^{13}C CP-MAS solid state NMR spectroscopy confirms the synthesis of chitosan containing guanidinium groups.

The spectrum of material **C**, *N*-guanidinium chitosan chloride, is given in figure 2b. Similarly to the spectrum of material **B**, a new signal at 160 ppm indicates the formation of guanidinium groups. The higher intensity of this signal indicates a higher guanylation degree in this material; the guanylation reactions seems to occur more efficiently in the presence of hydrochloric acid.

Figure 2 d/e shows the ^{13}C CP-MAS solid state NMR for *N*-guanidinium chitosan *(N, N′*-dicyclohexyl) acetate **D** and *N*-guanidinium chitosan (*N*-(3-Dimethylaminopropyl)-N'-ethyl hydrochloride **E**. In both spectra, additional signals, in the region between 20 – 45 ppm, indicate the presence of aliphatic carbon centers, originate from the grafting of the carbodiimides on the amine groups of the chitosan chains. Furthermore, the signals of the carbons center of the guanidinium groups around 160 ppm can also be seen in both spectra.

^{13}C CP-MAS solid state NMR spectroscopy therefore gives clear evidence for the successful guanylation of the chitosan scaffold. Both reaction strategies, guanylation with cyanamide in acidic reaction media (acetic or hydrochloric acid), or the use of aliphatic carbodiimides, allow for a successful functionalization of the chitosan scaffold with either unsubstituted of alkylated guanidinium groups.

3.4. TGA

The thermogravimetric analysis (TGA) curves for chitosan **A** and its derivatives **B** - **E** over the 30-800°C range, are displayed in figure 3. In all materials, the weight losses can be separated into three main temperature regions, designed as regions I, II and III. From room temperature to 120°C (region I), the weight loss ranging from 0.4 to 8.1%, may be attributed to the evaporation of physically adsorbed water. The amount of

physically adsorbed water is significantly higher in chitosan derivatives containing acetate anions compared to N-guanidinium chitosan chloride. This difference may be due to the higher hydrophilicity of chitosan derivatives containing acetate anion with the same compound containing chloride anions. In region II (120 – 300°C), a sharp weight loss indicates the thermal degradation of chitosan scaffolds. The degradation temperature at 80% weight loss follows the ascending order: **A** (279) ~ **B** (278) < **D** (258) < **C** (250) < **E** (242), showing that the guanylated chitosan materials in general show a lower thermal stability compared to the parent neat chitosan. The thermograms show only slight differences which confirm that the thermal stability of chitosan derivatives is close to the thermal behavior of neat chitosan. These results also show that the crystal structure of neat chitosan has not been completely destroyed via dissolution and regeneration even in acidic aqueous solutions or in ionic liquids.

Finally, at temperatures above 300°C, we observed a complete decomposition of the materials. The third weight loss, region III (300 – 700°C), recorded high stability for N-guanidinium chitosan chloride comparing with neat chitosan and other derivatives. For example, the weight loss% reached 81.9, 77.5, 70.8, 84.8, 81.5% for the materials A, B, C, D and E, respectively, at 550 °C.

3.5. Antimicrobial activity

The antimicrobial activity of the materials could be evaluated through various protocols depending on the solubility performance of the assayed samples. During this study, the antimicrobial activity of chitosan and its new derivatives was estimated through two techniques, the minimal inhibitory concentration (MIC) and the time required for killing. The MIC test was estimated through turbidimetric technique using different concentrations, from 100 to zero mg/ml (The results were presented in tables S1 to S5). Figure 4 displays the statistical analysis of the MICs results for the all materials (**A**, **B**, **C**, and **D**). Chitosan **A** displays low antimicrobial activity in comparison with the new derivatives, especially with Gram negative bacteria. The MICs values of chitosan recorded 25 mg/mL for Escherichia *coli* (NCTC-10416), *Staphylococcus aureus* (NCTC-7447), *Bacillus subtilis* (NCID-3610), *Candida albicans* (NCCLS 11) and 50 mg/mL for *Pseudomonas aeruginosa* (NCID-9016). Further studies displayed that the MIC of chitosan films for gram-negative was almost 200 mg/ml and for gram-positive was 40 mg/ml (Takahashi, Imai, Suzuki, & Sawai, 2008). Another studies showed that MIC values of chitosan for most gram negative

11

bacteria was around 100 to 10 mg/ml (Helander, Nurmiaho-Lassila, Ahvenainen, Rhoades, & Roller, 2001; Tsai, Wu, & Su, 2000). Moreover, several studies described the creation of various active groups on the chitosan backbone to support and extend its antimicrobial activity (Avadi et al., 2004; Shehabeldine & Hasanin, 2019).

It is well known that the chitosan antimicrobial activity arises from the action of the two electron lone pairs presented in the amino groups. These groups react with microorganism cell wall via complexion reaction which produced choppy microorganism wall (Shehabeldine & Hasanin, 2019). However, the antimicrobial activity of the novel materials (B to E) increased significantly compared to chitosan which can be attributed to the formed guanidinium groups. These groups are cationic and can enhance the permeability of cytoplasmic membrane via adsorption and bonding to intracellular constituents and kills the organisms. Moreover, the cell membrane disorganization and pore formation disrupt the cells permeability mechanisms. Also, the guanidine compounds effect on DNA and cellular proteins of bacteria (Zhou, Wei, Guan, Zheng, & Zhong, 2010).

More specifically, *N*-guanidinium chitosan acetate **B** exhibited the highest antimicrobial activity as shown in figure 4. This material showed the lowest MICs value (less than 3.125 mg/ml) with all assayed organisms which refers to its effective broad spectrum antimicrobial activity. This high value of reactivity arises from the presence of anionic acetate counter ion which also possesses inherited antimicrobial activity (Cacic, Trkovnik, Cacic, & Has-Schon, 2006; Chung, Lee, & Kim, 1998). In this context, the samples **C**, **D** and **E** showed intermediate antimicrobial activity against all assayed microorganisms which is still higher compared to chitosan. The novel derivatives recorded the following order: **C** > **E** > **D**. However, material **C** has high antimicrobial reactivity comparing the other two materials, **D** and **E**. This observation may be due to the delocalization of the positive charge on guanidinium groups via the alky chains in the materials **D** and **E**. Moreover, the free mobility of Cl$^-$ atom in material **C** improved its antimicrobial activity (Kim, Pitts, Stewart, Camper, & Yoon, 2008). Material **D,** therefore, exhibited the lowest antimicrobial activity among the investigated samples. These results may be due to special structure of material **D** which contains two bulky cyclohexyl groups. These groups act as a barrier for interactions between the new derivative and the cell wall (Malík et al., 2016).

Consequently, the time required for killing was calculated considering chitosan as reference sample and *N*-guanidinium chitosan acetate **B** as the highest antimicrobial derivative and DMSO as blank. **Figure 5** shows the surviving of assayed microorganisms against time during treatment with chitosan, material **B** and DMSO. The native chitosan displays the long time for treatment with *Escherichia coli* (NCTC-10416), *Pseudomonas aeruginosa* (NCID-9016), *Staphylococcus aureus* (NCTC-7447), *Bacillus subtilis* (NCID-3610) and *Candida albicans* (NCCLS 11) by 16, 20, 20, 18 and 18 hours, respectively. The rate of killing in case of material **B** was reduced to 12, 10, 12, 14, and 12 hours for *Escherichia coli* (NCTC-10416), *Pseudomonas aeruginosa* (NCID-9016), *Staphylococcus aureus* (NCTC-7447), *Bacillus subtilis* (NCID-3610) and *Candida albicans* (NCCLS 11). Material **B** showed a synergetic effect arising from both guanidinium groups and anionic acetate which enhanced the rate of microbial cells destruction (M. Hasanin, El-Henawy, Eisa, El-Saied, & Sameeh, 2019; M. S. Hasanin & Moustafa, 2020). Overall, the novel derivatives have excellent antimicrobial activity with high rate of microorganisms killing. Therefore, the new derivatives from **B** - **E** can be considered as broad spectrum antimicrobial agents. Using different bioassay will be required for complete picture of the antimicrobial action of the novel materials (Houghton, Howes, Lee, & Steventon, 2007).

4. Conclusion

New chitosan derivatives bearing guanidinium functions were synthesized by direct reaction between chitosan and either cyanamide in aqueous medium or carbodiimides in ionic liquid media. The new derivatives exhibited high broad spectrum antimicrobial activity. Among the new materials, *N*-guanidinium chitosan acetate showed the highest antimicrobial activity with high rate of killing according to the time required for killing test. *N*-guanidinium chitosan acetate recorded low value of MIC toward all microbial strains. The antimicrobial evaluation of the new derivatives showed an effective inhibition against various bacterial strains of *Escherichia coli* (NCTC-

10416), *Pseudomonas aeruginosa* (NCID-9016), *Staphylococcus aureus* (NCTC-7447), *Bacillus subtilis* (NCID-3610) and *Candida albicans* (NCCLS 11) which demonstrated their applications in the area of biomaterials.

Author Statement

Ahmed Salama and Peter Hesemann developed the polymer synthesis and designed the experiments. They shared equally in data curation, funding acquisition, investigation, project administration, resources, software and writing. Mohamed Hasanin assayed the antimicrobial study. All authors commented on the manuscript and supported data analysis.

Notes:

References.

Avadi, M. R., Sadeghi, A. M. M., Tahzibi, A., Bayati, K., Pouladzadeh, M., Zohuriaan-Mehr, M. J., & Rafiee-Tehrani, M. (2004). Diethylmethyl chitosan as an antimicrobial agent: Synthesis, characterization and antibacterial effects. *European Polymer Journal*, *40*(7), 1355–1361. https://doi.org/10.1016/j.eurpolymj.2004.02.015

Balouiri, M., Sadiki, M., & Ibnsouda, S. K. (2016). Methods for in vitro evaluating antimicrobial activity: A review. *Journal of Pharmaceutical Analysis*, *6*(2), 71–79. https://doi.org/10.1016/j.jpha.2015.11.005

Cacic, M., Trkovnik, M., Cacic, F., & Has-Schon, E. (2006). Synthesis and Antimicrobial Activity of Some Derivatives on the Basis (7-hydroxy-2-oxo-2H-chromen-4-yl)-acetic Acid Hydrazide. *Molecules*, *11*(2), 134–147. https://doi.org/10.3390/11010134

Cao, Y., Du, Z., Li, W., Li, J., Zhang, Y., Xu, F., & Shen, Q. (2011). Activation of Carbodiimide and Transformation with Amine to Guanidinate Group by Ln(OAr) 3 (THF) 2 (Ln: Lanthanide and Yttrium) and Ln(OAr) 3 (THF) 2 as a Novel Precatalyst for Addition of Amines to Carbodiimides: Influence of Aryloxide Group. *Inorganic Chemistry*, *50*(8), 3729–3737. https://doi.org/10.1021/ic200091s

Chung, Y.-S., Lee, K.-K., & Kim, J.-W. (1998). Durable Press and Antimicrobial Finishing of Cotton Fabrics with a Citric Acid and Chitosan Treatment. *Textile Research Journal*, *68*(10), 772–775. https://doi.org/10.1177/004051759806801011

Eid, I., Elsebaei, M. M., Mohammad, H., Hagras, M., Peters, C. E., Hegazy, Y. A., … Mayhoub, A. S. (2017). Arylthiazole antibiotics targeting intracellular methicillin-resistant Staphylococcus aureus (MRSA) that interfere with bacterial cell wall synthesis. *European Journal of Medicinal Chemistry*, *139*, 665–673. https://doi.org/10.1016/j.ejmech.2017.08.039

Hasanin, M., El-Henawy, A., Eisa, W. H., El-Saied, H., & Sameeh, M. (2019). Nano-amino acid cellulose derivatives: Eco-synthesis, characterization, and antimicrobial properties. *International Journal of Biological Macromolecules*, *132*, 963–969. https://doi.org/10.1016/j.ijbiomac.2019.04.024

Hasanin, M. S., & Moustafa, G. O. (2020). New potential green, bioactive and antimicrobial nanocomposites based on cellulose and amino acid. *International Journal of Biological Macromolecules*, *144*, 441–448. https://doi.org/10.1016/j.ijbiomac.2019.12.133

Hassan, H., Salama, A., El-ziaty, A. K., & El-sakhawy, M. (2019). International Journal of Biological Macromolecules New chitosan / silica / zinc oxide nanocomposite as adsorbent for dye removal. *International Journal of Biological Macromolecules*, *131*, 520–526. https://doi.org/10.1016/j.ijbiomac.2019.03.087

Helander, I. ., Nurmiaho-Lassila, E.-L., Ahvenainen, R., Rhoades, J., & Roller, S. (2001). Chitosan disrupts the barrier properties of the outer membrane of Gram-negative bacteria. *International Journal of Food Microbiology*, *71*(2–3), 235–244. https://doi.org/10.1016/S0168-1605(01)00609-2

Holappa, J., Nevalainen, T., Savolainen, J., Soininen, P., Elomaa, M., Safin, R., … Järvinen, T. (2004). Synthesis and Characterization of Chitosan N -Betainates

Having Various Degrees of Substitution. *Macromolecules*, *37*(8), 2784–2789. https://doi.org/10.1021/ma0358780

Houghton, P. J., Howes, M. J., Lee, C. C., & Steventon, G. (2007). Uses and abuses of in vitro tests in ethnopharmacology: Visualizing an elephant. *Journal of Ethnopharmacology*, *110*(3), 391–400. https://doi.org/10.1016/j.jep.2007.01.032

Hu, Y., Du, Y., Yang, J., Kennedy, J. F., Wang, X., & Wang, L. (2007). Synthesis, characterization and antibacterial activity of guanidinylated chitosan. *Carbohydrate Polymers*, *67*(1), 66–72. https://doi.org/10.1016/j.carbpol.2006.04.015

Kim, J., Pitts, B., Stewart, P. S., Camper, A., & Yoon, J. (2008). Comparison of the Antimicrobial Effects of Chlorine, Silver Ion, and Tobramycin on Biofilm. *Antimicrobial Agents and Chemotherapy*, *52*(4), 1446–1453. https://doi.org/10.1128/AAC.00054-07

Malík, I., Csöllei, J., Jampílek, J., Stanzel, L., Zadražilová, I., Hošek, J., … O'Mahony, J. (2016). The Structure–Antimicrobial Activity Relationships of a Promising Class of the Compounds Containing the N-Arylpiperazine Scaffold. *Molecules*, *21*(10), 1274. https://doi.org/10.3390/molecules21101274

Monier, M., Abdel-Latif, D. A., & Youssef, I. (2018). Preparation of ruthenium (III) ion-imprinted beads based on 2-pyridylthiourea modified chitosan. *Journal of Colloid and Interface Science*, *513*, 266–278. https://doi.org/10.1016/j.jcis.2017.11.004

Sahariah, P., Benediktssdóttir, B. E., Hjálmarsdóttir, M. Á., Sigurjonsson, O. E., Sørensen, K. K., Thygesen, M. B., … Másson, M. (2015). Impact of Chain Length on Antibacterial Activity and Hemocompatibility of Quaternary *N* -Alkyl and *N* , *N* -Dialkyl Chitosan Derivatives. *Biomacromolecules*, *16*(5), 1449–1460. https://doi.org/10.1021/acs.biomac.5b00163

Sahariah, P., & Másson, M. (2017). Antimicrobial Chitosan and Chitosan Derivatives: A Review of the Structure-Activity Relationship. *Biomacromolecules*, *18*(11), 3846–3868. https://doi.org/10.1021/acs.biomac.7b01058

Sahariah, P., Másson, M., & Meyer, R. L. (2018). Quaternary Ammoniumyl Chitosan Derivatives for Eradication of Staphylococcus aureus Biofilms. *Biomacromolecules*, *19*(9), 3649–3658.

https://doi.org/10.1021/acs.biomac.8b00718

Salama, A. (2017). Dicarboxylic cellulose decorated with silver nanoparticles as sustainable antibacterial nanocomposite material. *Environmental Nanotechnology, Monitoring & Management*, *8*, 228–232. https://doi.org/10.1016/j.enmm.2017.08.003

Salama, A. (2018). Chitosan based hydrogel assisted spongelike calcium phosphate mineralization for in-vitro BSA release. *International Journal of Biological Macromolecules*, *108*, 471–476. https://doi.org/10.1016/j.ijbiomac.2017.12.035

Salama, A. (2019). Cellulose/calcium phosphate hybrids: New materials for biomedical and environmental applications. *International Journal of Biological Macromolecules*, *127*, 606–617. https://doi.org/10.1016/j.ijbiomac.2019.01.130

Salama, A., Abou-Zeid, R. E., Cruz-Maya, I., & Guarino, V. (2020). Soy protein hydrolysate grafted cellulose nanofibrils with bioactive signals for bone repair and regeneration. *Carbohydrate Polymers*, *229*(August 2019), 115472. https://doi.org/10.1016/j.carbpol.2019.115472

Salama, A., & El-Sakhawy, M. (2014). Preparation of polyelectrolyte/calcium phosphate hybrids for drug delivery application. *Carbohydrate Polymers*, *113*, 500–506. https://doi.org/10.1016/j.carbpol.2014.07.022

Salama, A., & Hesemann, P. (2018a). New N-guanidinium chitosan/silica ionic microhybrids as efficient adsorbent for dye removal from waste water. *International Journal of Biological Macromolecules*, *111*, 762–768. https://doi.org/10.1016/j.ijbiomac.2018.01.049

Salama, A., & Hesemann, P. (2018b). Synthesis of N-Guanidinium-chitosan/silica hybrid composites: Efficient adsorbents for anionic pollutants. *Journal of Polymers and the Environment*, *26*(5), 1986–1997. https://doi.org/10.1007/s10924-017-1093-3

Salama, A., & Hesemann, P. (2020). Synthesis and characterization of N -guanidinium chitosan / silica ionic hybrids as templates for calcium phosphate mineralization. *International Journal of Biological Macromolecules*, *147*, 276–283. https://doi.org/10.1016/j.ijbiomac.2020.01.046

Shehabeldine, A., & Hasanin, M. (2019). Green synthesis of hydrolyzed starch–chitosan nano-composite as drug delivery system to gram negative bacteria. *Environmental Nanotechnology, Monitoring & Management*, *12*, 100252–100260. https://doi.org/10.1016/j.enmm.2019.100252

Short, J. H., & Darby, T. D. (1967). Sympathetic nervous system blocking agents. 3. Derivatives of benzylguanidine. *Journal of Medicinal Chemistry*, *10*(5), 833–840.

Takahashi, T., Imai, M., Suzuki, I., & Sawai, J. (2008). Growth inhibitory effect on bacteria of chitosan membranes regulated with deacetylation degree. *Biochemical Engineering Journal*, *40*(3), 485–491. https://doi.org/10.1016/j.bej.2008.02.009

Tsai, G.-J., Wu, Z.-Y., & Su, W.-H. (2000). Antibacterial activity of a chitooligosaccharide mixture prepared by cellulase digestion of shrimp chitosan and its application to milk preservation. *Journal of Food Protection*, *63*(6), 747–752. https://doi.org/10.4315/0362-028X-63.6.747

Tsubokura, K., Iwata, T., Taichi, M., Kurbangalieva, A., Fukase, K., Nakao, Y., & Tanaka, K. (2014). Direct guanylation of amino groups by cyanamide in water: Catalytic generation and activation of unsubstituted carbodiimide by scandium(iii) triflate. *Synlett*, *25*(9), 1302–1306. https://doi.org/10.1055/s-0033-1341080

Vidar Rúnarsson, Ö., Holappa, J., Malainer, C., Steinsson, H., Hjálmarsdóttir, M., Nevalainen, T., & Másson, M. (2010). Antibacterial activity of N-quaternary chitosan derivatives: Synthesis, characterization and structure activity relationship (SAR) investigations. *European Polymer Journal*, *46*(6), 1251–1267. https://doi.org/10.1016/j.eurpolymj.2010.03.001

Wiarachai, O., Thongchul, N., Kiatkamjornwong, S., & Hoven, V. P. (2012). Surface-quaternized chitosan particles as an alternative and effective organic antibacterial material. *Colloids and Surfaces B: Biointerfaces*, *92*, 121–129. https://doi.org/10.1016/j.colsurfb.2011.11.034

Zhang, X., Duan, Y., Wang, D., & Bian, F. (2015). Preparation of arginine modified PEI-conjugated chitosan copolymer for DNA delivery. *Carbohydrate Polymers*, *122*, 53–59. https://doi.org/10.1016/j.carbpol.2014.12.054

Zhou, Z. X., Wei, D. F., Guan, Y., Zheng, A. N., & Zhong, J. J. (2010). Damage of Escherichia coli membrane by bactericidal agent polyhexamethylene guanidine

hydrochloride: micrographic evidences. *Journal of Applied Microbiology*, *108*(3), 898–907. https://doi.org/10.1111/j.1365-2672.2009.04482.x
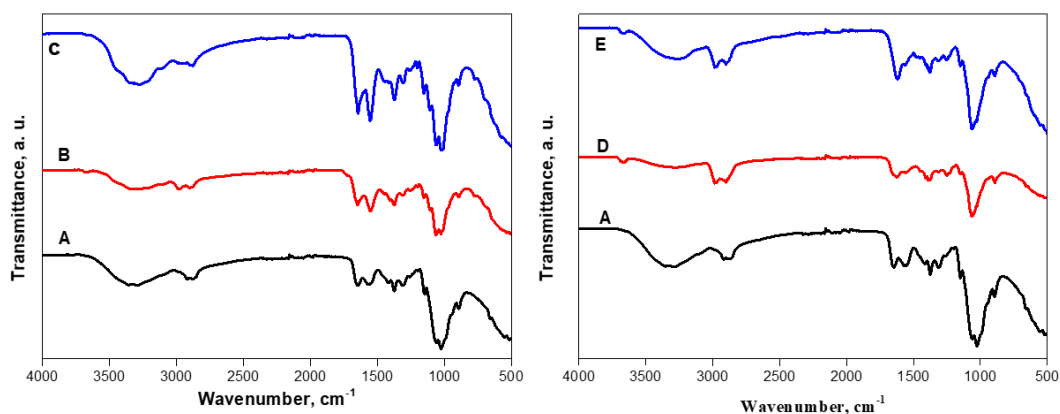
Figure 1: FT-IR study of chitosan and its derivatives B, C, D and E
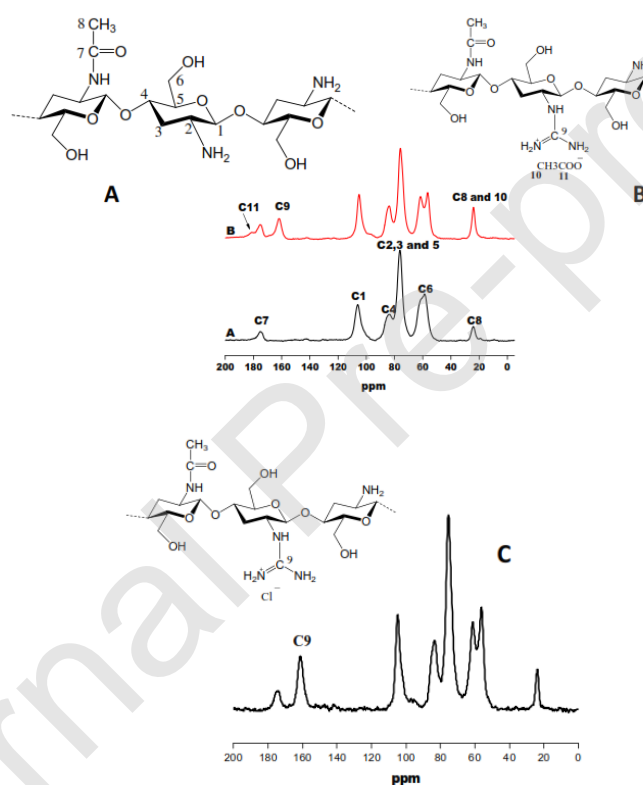

Figure 2a/b/c: ^{13}C CP-MAS solid state NMR for chitosan **A**, *N*-guanidinium chitosan acetate **B** (*left*) and *N*-guanidinium chitosan chloride **C** (*right*).
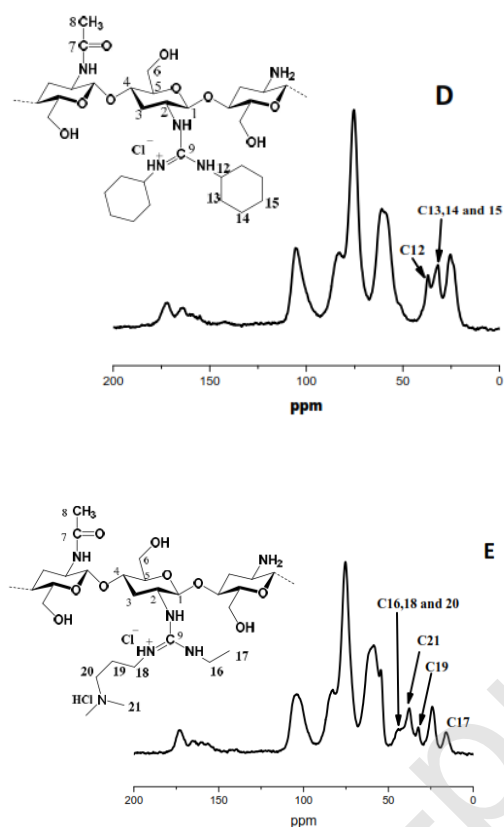
20

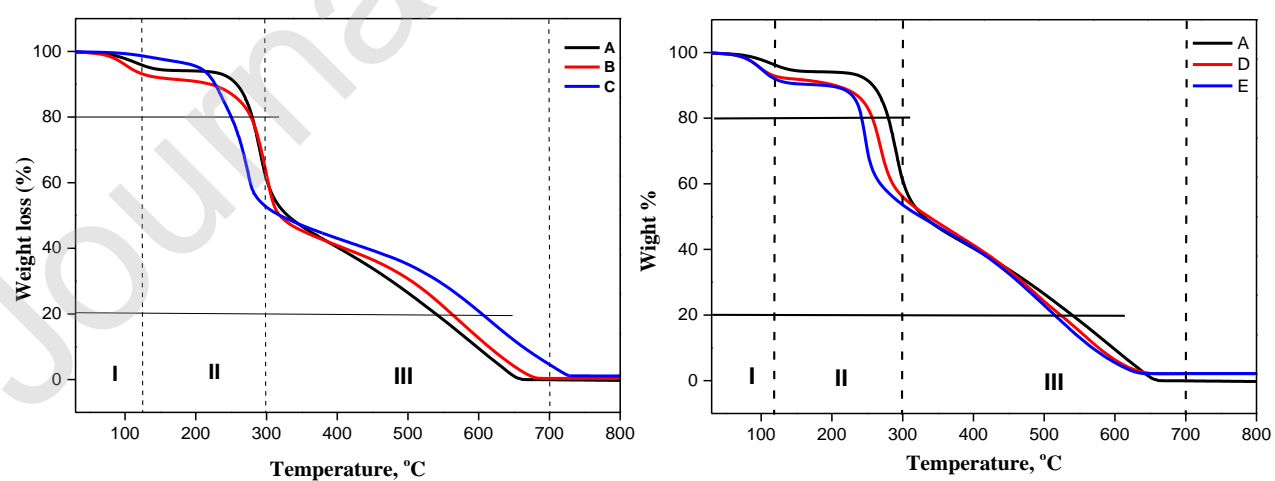Figure 2d/e: ^{13}C CP-MAS solid state NMR for N-guanidinium chitosan *(derivatives D and E)*.

Figure 3: TGA of chitosan **A** and its derivatives **B**, **C**, **D** and **E** (under air flux, heating ramp 5°C/min)
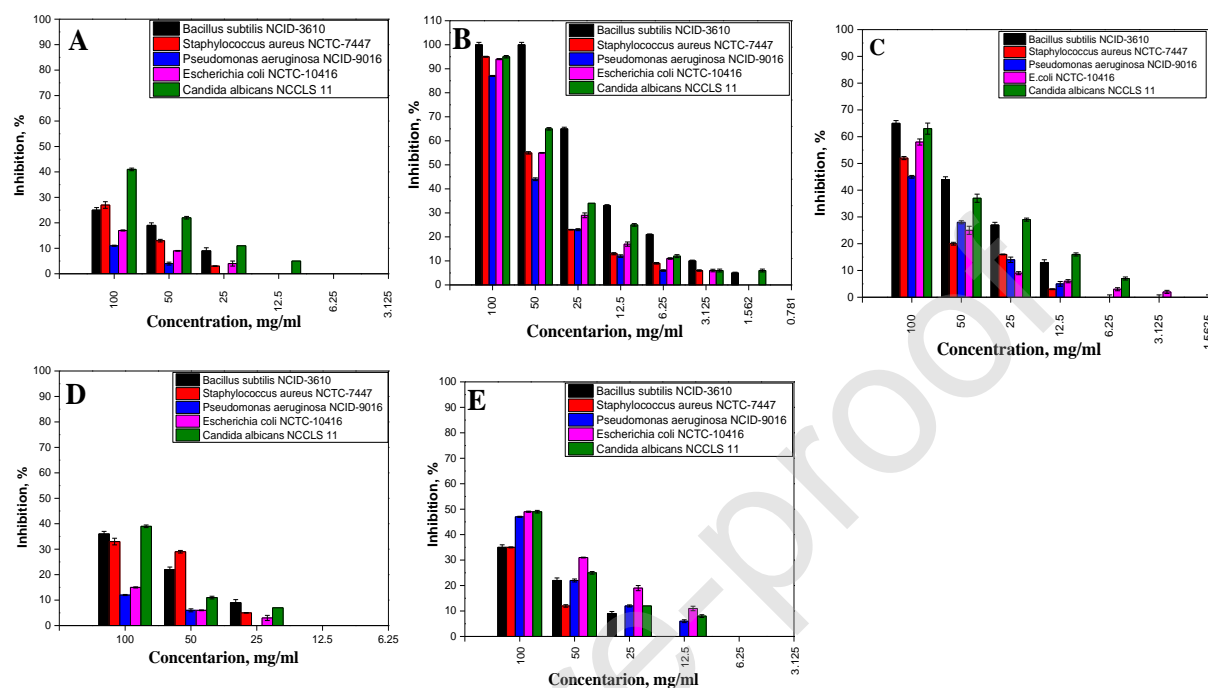

Figure 4: Statistical analysis of MIC for samples **A**, B, **C**, **D** and **E** against *E. coli*, *P.aeruginosa, S. aureus, B. subtilis* and *C.albicans*.

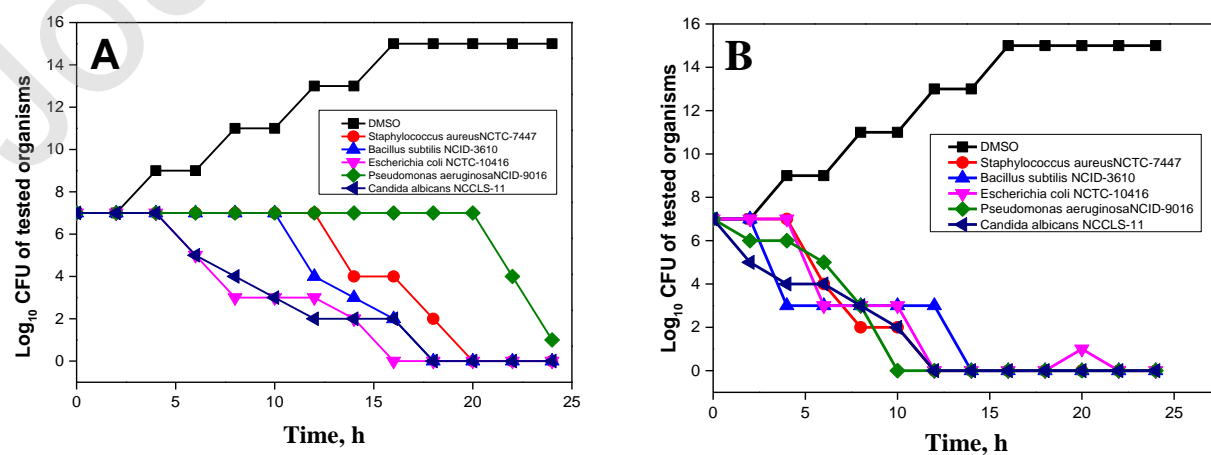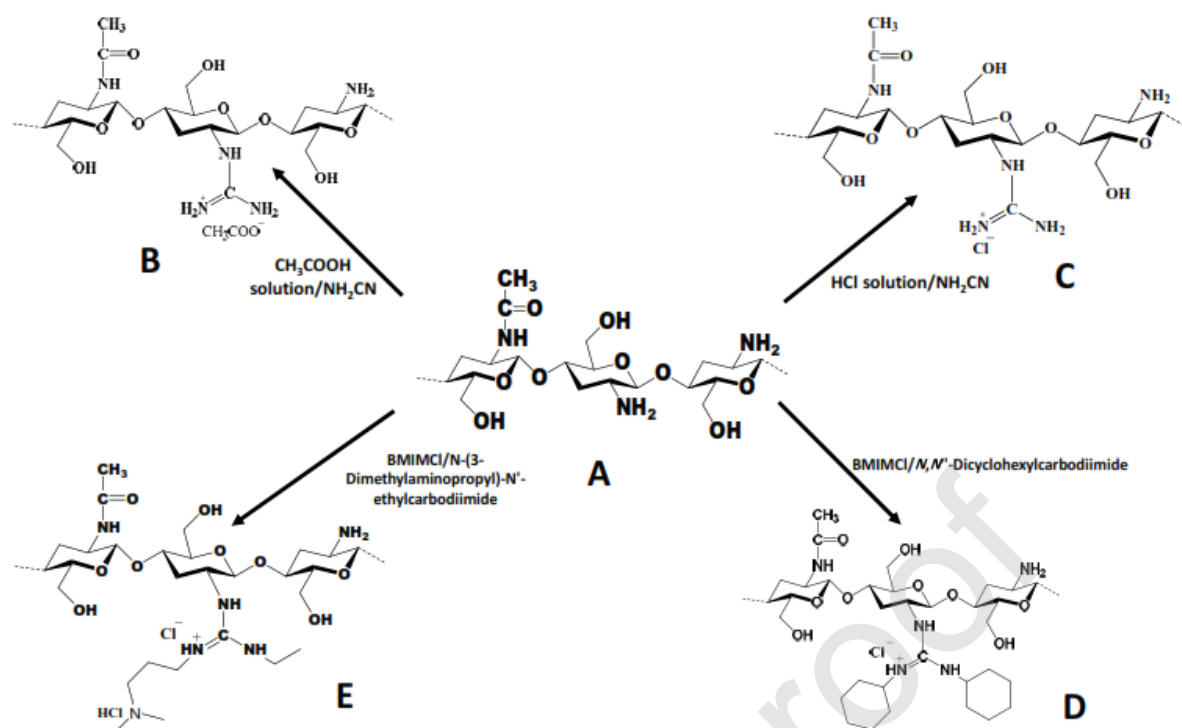**Figure 5:** Time required for killing (*E. coli*, *P. aeruginosa, S. aureus, B. subtilis* and *C. albicans*.) for **A** and **C**.

Scheme 1: Synthesis of *N*-guanidinium chitosan derivatives

Table 1: Elemental analysis of chitosan (A) and its derivatives (B, C, D and E).

Samples	C[%]	H[%]	N[%]
A	43.06±0.02	6.73±0.07	7.7±0.13
B	41.34±0.42	6.48±0.21	11.06±0.07
C	34.0±0.3	6.21±0.24	12.33±0.17
D	39.31±0.23	6.84±0.28	7.06±0.17
E	36.57±0.24	8.24±0.13	10.47±0.01